Submitted to IDETC/CIE 2006
ASME 2006 International Design Engineering Technical Conferences
and Computers and Information in Engineering Conference
September 10-13, 2006, Philadelphia, Pennsylvania, USA

DETC2006-99177

THREE-CABLE HAPTIC INTERFACE

Robert L. Williams II, Venkat Chadaram, and **Federica Giacometti**
Department of Mechanical Engineering, Ohio University, Athens, Ohio 45701
williar4@ohio.edu

ABSTRACT
We present our three-cable haptic interface (TCHI) concept, plus modeling and simulation, hardware implementation, and initial experimental results. This device is based on a previous system developed by Italian researchers. Cable devices are limited since they cannot push on the user, but only apply positive tension. In addition, this TCHI is further limited since it has no actuation redundancy and forces can only be applied within the tetrahedron formed by the fingertip point and base cable attachment points. Despite these limitations, which are explored herein, we believe the simplicity of this haptic interface can make it a serious competitor of existing commercial devices in terms of workspace, force application, cost, safety, and stiffness.

KEYWORDS
Cable-suspended haptic interface, feasible force, virtual reality, palpatory training

INTRODUCTION
Haptic interfaces provide a sense of wrench (force/moment) and/or tactile feedback to the human from computer-simulated or remote environments. Most existing haptic devices are too heavy, strong, expensive, and not dexterous enough to achieve widespread application. Compared to most commercial devices, cable-suspended haptic interfaces (CSHIs, such as the devices from Italy shown in Figures 1 and 2) have intriguing potential benefits. Cable-suspended robots (CSRs) are a type of parallel manipulators wherein the end-effector link is supported in-parallel by *n* cables with *n* tensioning motors. In addition to the well-known advantages of parallel manipulators relative to serial manipulators, cable-based systems can have lower mass and far better workspaces than other parallel manipulators. Pioneers in CSRs include Albus et al. (1993) and Campbell et al. (1995).

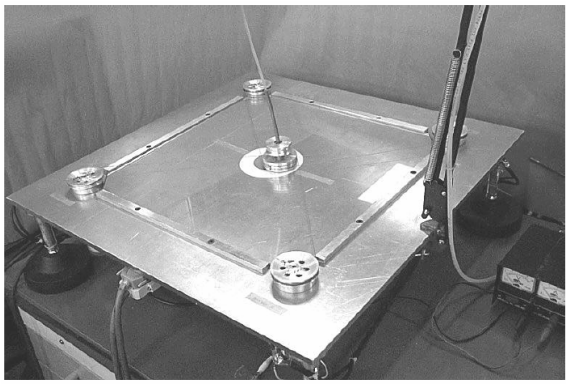

Figure 1. Feriba-3 Four-Cable Planar Haptic Device (Gallina et al., 2001)

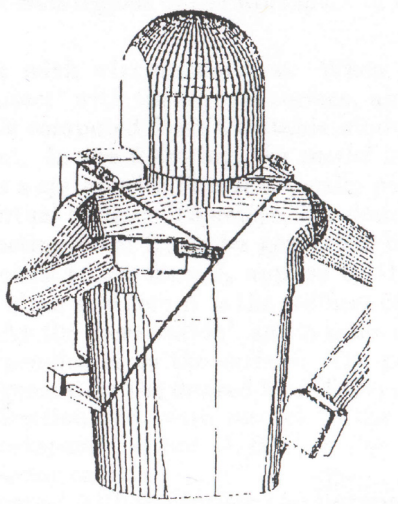

Figure 2. WireMan Cable-Suspended Haptic Interface (Bonivento et al., 1997)

Several CSHIs have been built and tested. Some of these are the Texas 9-string (Lindemann and Tesar, 1989), the SPIDAR (Ishii and Sato, 1994), the 7-cable master (Kawamura

and Ito, 1993) and the 8-cable haptic interface (Williams, 1998). According to its authors, the Texas 9-string device was bulky, suffered from cable interface, and failed to provide small feed back forces due to large actuator friction. Also, the band width was low, which resulted in large time delays and jerky motion. The SPIDAR system was developed with four strings to give force reflection to a single operator fingertip. It was extended to eight strings to include thumb feedback (Walairacht et al., 1999).

CSRs and CSHIs can be made lighter, stiffer, safer, and more economical than traditional serial robots and haptic interfaces since their primary structure consists of lightweight, high load-bearing cables. On the other hand, one major disadvantage is that cables can only exert tension and cannot push on the end-effector, i.e. negative cable tensions must be avoided. Williams and Gallina (2002) developed a dynamic model to determine the wrench-exertion workspace (with only positive cable tensions) and a method to control for only positive cable tensions.

Gallina et al. (2001) developed the Feriba-3 (Figure 1), a 4-wire mechanism with a circular end-effector spool. Each wire is fixed to the lateral side of the spool and can wind around the spool. Their particular geometric configuration made the system manipulable inside a large workspace and the kinematic forward and reverse pose solutions closed-form. Brau et al. (2005) present singularity-free CSHIs.

All of the above systems have actuation redundancy, i.e. more active cables than the number of degrees of freedom they provide. Bonivento et al. (1997) developed a cable driven haptic interface without actuation redundancy, the WireMan (Figure 2). This is a three-wire-driven haptic interface allowing three Cartesian translations with three Cartesian forces for the exploration of virtual surfaces. The WireMan is a portable haptic interface as shown with a thimble for the operator's finger. With this sort of configuration it is possible to apply Cartesian forces only which are directed inside the tetrahedron formed by the three wires and base. They also evaluated a performance index for this device which is 3D space defective due to the lack of actuation redundancy. Farahani and Ryu (2005) developed a wearable three-cable haptic interface, the HapticPen, inspired by the Wireman.

The current paper presents our three-cable haptic interface (TCHI) designed and built at Ohio University, based on the concept of the WireMan. Our workspace and force design specifications were based on the commercial PHANToM 3.0 haptic interface – our work is still in progress and hence we do not yet make a comparison with that device. Though the TCHI forces are limited due to lack of actuation redundancy, the kinematics and statics Jacobian solutions are easily derived in closed-form. Also, the feasible forces directed toward the user make this TCHI suitable for application in the Virtual Haptic Back Project at Ohio University (Williams et al., 2004a). The purpose of that project is to train physicians in palpatory diagnosis (identifying medical problems via touch), currently focusing on the human spine and back.

This paper is organized as follows. The next section describes our TCHI concept, then we present closed-form kinematics and statics modeling and solutions, followed by some simulation examples. We end with a description of our hardware and controller, with some preliminary experimental results.

THREE-CABLE HAPTIC INTERFACE CONCEPT

This section describes our Three-Cable Haptic Interface (TCHI) concept, inspired by WireMan (Figure 2, Bonivento et al., 1997). For now our system is fixed to the table. As mentioned earlier we used the PHANToM® 3.0 haptic interface for design specifications. Figure 3 shows our TCHI diagram. The base Cartesian reference frame is {0}, attached and directed as shown. Each of the three cables is passed through the ground link at the fixed-base cable points ${}^0\mathbf{B}_1 = \{-L_x \quad 0 \quad 0\}^T$, ${}^0\mathbf{B}_2 = \{0 \quad 0 \quad 0\}^T$, ${}^0\mathbf{B}_3 = \{0 \quad 0 \quad -L_z\}^T$. The active cable lengths are $\mathbf{L} = \{L_1 \quad L_2 \quad L_3\}^T$. The vector ${}^0\mathbf{P} = \{x \quad y \quad z\}^T$ gives the position of finger tip with respect to the {0} origin, expressed in {0} coordinates. The active cable tensions are $\mathbf{T} = \{t_1 \quad t_2 \quad t_3\}^T$ and the resultant Cartesian fingertip force is ${}^0\mathbf{F}_r = \{f_x \quad f_y \quad f_z\}^T$. The finger thimble is located at ${}^0\mathbf{P}$ and the three tensioning motors reels are mounted at ${}^0\mathbf{B}_i$, controlling the active cable tensions $\mathbf{T}$ to achieve the desired Cartesian fingertip force ${}^0\mathbf{F}_r$ for haptic feedback.

There is no actuation redundancy since there are three active cable tensions for three Cartesian force components. Hence we can exert only ${}^0\mathbf{F}_r$ contained within all three positive cable tensions; that is, within the tetrahedron $B_1B_2B_3P$ since cables may exert only tension. This force limitation is configuration-dependent. The largest force magnitudes can be directed back towards the user. Generally smaller force magnitudes are possible in transverse directions. This limited haptic feedback is well suited for most haptic needs in the Virtual Haptic Back project at Ohio University (Williams et al., 2004).

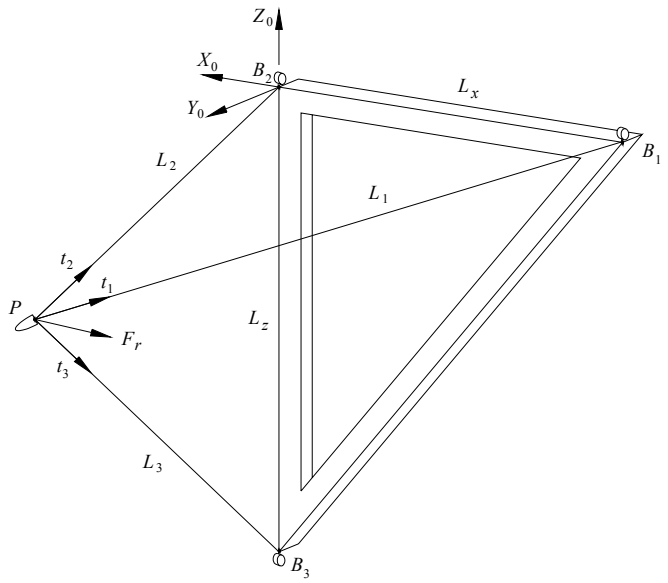

Figure 3. Three-Cable Haptic Interface Diagram

KINEMATICS AND STATICS

This section presents our closed-form kinematics and statics modeling and solutions for simulation and control of the three-cable haptic interface (TCHI).

Kinematics

Kinematics modeling is concerned with relating the Cartesian position of the fingertip to the three cable lengths.

Inverse Position Kinematics. The inverse pose kinematics (IPK) problem is stated: Given the desired finger tip position ${}^0\mathbf{P}$, calculate the three active cable lengths **L**. Like most CSRs and CSHIs, the inverse pose kinematics problem is straight-forward since the cable lengths are simply the Euclidean norms of the cable vectors connecting each base point with the fingertip:

$$L_i = \left\| {}^0\mathbf{B}_i - {}^0\mathbf{P} \right\| \qquad i = 1,2,3 \tag{1}$$

$$\begin{aligned} L_1 &= \sqrt{x^2 + y^2 + z^2 + L_x^2 + 2L_x x} \\ L_2 &= \sqrt{x^2 + y^2 + z^2} \\ L_3 &= \sqrt{x^2 + y^2 + z^2 + L_z^2 + 2L_z z} \end{aligned} \tag{2}$$

Substituting the specific cable base point parameters in {0}, we see the IPK solution (2) is simple. The IPK solution may be used in simulation, it is not required for on-line operation of the TCHI.

Forward Position Kinematics. The forward position kinematics (FPK) problem is stated: Given the three active cable lengths **L**, calculate the Cartesian position of the fingertip ${}^0\mathbf{P}$. This position is then implemented in real-time for haptics applications. That is, as the human moves, the motor encoders read **L**, and FPK sends the user position ${}^0\mathbf{P}$ to the virtual world.

The FPK solution consists of finding the intersection point of three given spheres. Let a sphere be referred as a vector center point **c** and scalar radius *r*: (**c**, *r*). The unknown point ${}^0\mathbf{P}$ is found as follows:

${}^0\mathbf{P}$ is the intersection of (${}^0\mathbf{B_1}$, L_1), (${}^0\mathbf{B_2}$, L_2), and (${}^0\mathbf{B_3}$, L_3)

Now the equations and solution for the intersection point ${}^0\mathbf{P} = \{x \quad y \quad z\}^T$ of the three above spheres are derived for our specific TCHI parameters. The equations of the above three spheres are:

$$\begin{aligned} \left(x + L_x\right)^2 + y^2 + z^2 &= L_1^2 \\ x^2 + y^2 + z^2 &= L_2^2 \\ x^2 + y^2 + \left(z + L_z\right)^2 &= L_3^2 \end{aligned} \tag{3}$$

Equations (3) are coupled nonlinear equations in the three unknowns *x*, *y* and *z*. The solution will yield the intersection point ${}^0\mathbf{P} = \{x \quad y \quad z\}^T$. The solution approach is to first expand the first and third terms of the first and the third equations of (3). Then subtract the second equation from first and third equations to find *x* and *z*. Then *y* is found from second equation of (3), once *x* and *z* are known. In this way we obtain the solution *x*, *y* and *z* as follows:

$$\begin{aligned} x &= \frac{L_1^2 - L_2^2 - L_x^2}{2L_x} \\ z &= \frac{L_3^2 - L_2^2 - L_z^2}{2L_z} \\ y &= \pm\sqrt{L_2^2 - x^2 - z^2} \end{aligned} \tag{4}$$

Mathematically there are two solutions to the intersection of three spheres in general. (*x*, *z*) is unique but there are two *y* values as shown in (4). However in the design shown in Figure 3, only the +*y* solution will be useful. Therefore, we have a unique FPK solution. Williams et al. (2004b) discuss the multiple solutions, algorithmic singularities, and imaginary solutions for the general three-spheres intersection algorithm. For the TCHI, imaginary solutions could be a problem only if the cable lengths are not sufficiently long to intersect at point ${}^0\mathbf{P}$. If the cable length sensing is good this will not happen. The algorithmic singularities may easily be avoided by proper choice of coordinates for the base cable points (Williams et al., 2004b). Due to the simple structure of the TCHI, our algorithmic singularities are simply $L_x = 0$ and $L_z = 0$, which are avoided by design.

So, the FPK derivation is straight-forward and a unique solution always exists assuming good cable sensing and non-

zero L_x and L_z. This FPK solution is critical to the real-time haptic interface implementation.

Statics

Since the cable and finger thimble mass is very small and assuming that human fingertip velocities and accelerations are relatively small, the TCHI may be controlled in a pseudostatic manner. In this subsection statics modeling is presented. These equations are used to simulate and program the TCHI to provide desired Cartesian forces to the fingertip.

Static Equilibrium. For the system to be in static equilibrium, the sum of tension forces exerted on the fingertip thimble must be equal to the resultant force exerted on the finger tip (the human finger must exert an equal and opposite force on the thimble for pseudostatic equilibrium). The statics equations are:

$$\sum_{i=1}^{3} \mathbf{t}_i = \sum_{i=1}^{3} t_i \, {}^0\hat{\mathbf{L}}_i = {}^0\mathbf{F}_r \tag{5}$$

Gravity is ignored because the weight of the fingertip thimble and cables are very small compared to the tension and resultant force levels. In equations (5), t_i is the cable tension applied to the i^{th} cable by its motor (in the cable length unit direction ${}^0\mathbf{L}_i$ directed from ${}^0\mathbf{P}$ to ${}^0\mathbf{B}_i$ because t_i must only be in tension); and ${}^0\mathbf{F_r}$ is the resultant vector force exerted on the fingertip by the haptic interface. Substituting the above terms into (5) yields:

$$ {}^0\mathbf{F}_r = {}^0\mathbf{A}\mathbf{T} \tag{6}$$

where $\mathbf{T} = \{t_1 \quad t_2 \quad t_3\}^T$ is the vector of scalar cable tensions, ${}^0\mathbf{F}_r$ is the resultant vector force (expressed in {0} coordinates), and the 3x3 statics Jacobian matrix ${}^0\mathbf{A}$ (expressed in {0} coordinates) is:

$$ {}^0\mathbf{A} = \left[{}^0\hat{\mathbf{L}}_1 \quad {}^0\hat{\mathbf{L}}_2 \quad {}^0\hat{\mathbf{L}}_3 \right] \tag{7}$$

The statics Jacobian matrix for the TCHI of Figure 3 is:

$$ {}^0\mathbf{A} = \begin{bmatrix} \dfrac{-L_x - x}{L_1} & \dfrac{-x}{L_2} & \dfrac{-x}{L_3} \\ \dfrac{-y}{L_1} & \dfrac{-y}{L_2} & \dfrac{-y}{L_3} \\ \dfrac{-z}{L_1} & \dfrac{-z}{L_2} & \dfrac{-L_z - z}{L_3} \end{bmatrix} \tag{8}$$

It is well known from the mechanics of parallel robots that given the statics Jacobian matrix, we can easily find the velocity kinematics that maps cable length rates into the Cartesian velocity of point P, ${}^0\dot{\mathbf{X}} = {}^0\mathbf{J}\dot{\mathbf{L}}$:

$$ {}^0\mathbf{J} = -{}^0\mathbf{A}^T \tag{9}$$

Pseudostatics Solution. The determinant of the statics Jacobian matrix ${}^0\mathbf{A}$ is:

$$ \left| {}^0\mathbf{A} \right| = \frac{-L_x L_z y}{L_1 L_2 L_3} \tag{10}$$

Assuming non-zero L_x and L_z, the only statics singularity condition is $y = 0$; when the fingertip is on the XZ plane ($y = 0$), it is impossible to exert f_y. Also, due to the duality with velocity, in this singularity condition it is impossible to control $\dot{y}$.

The statics equations (6) can be inverted (as long as $y \neq 0$) in an attempt to exert general Cartesian forces ${}^0\mathbf{F}_r$ with cable tensions $\mathbf{T}$:

$$ \{\mathbf{T}\} = \left[{}^0\mathbf{A}^{-1} \right] \{ {}^0\mathbf{F}_r \} \tag{11}$$

where

$$ {}^0\mathbf{A}^{-1} = \begin{bmatrix} \dfrac{-L_1}{L_x} & \dfrac{L_1 x}{L_x y} & 0 \\ \dfrac{L_2}{L_x} & \dfrac{-L_2 \left(L_z x + L_x z + L_x L_z \right)}{L_x L_z y} & \dfrac{L_2}{L_z} \\ 0 & \dfrac{L_3 z}{L_z y} & \dfrac{-L_3}{L_z} \end{bmatrix} \tag{12}$$

So we have a closed-form solution to the cable tensions $\mathbf{T}$ given ${}^0\mathbf{F}_r$:

$$\begin{aligned} t_1 &= \frac{-L_1}{L_x} f_x + \frac{L_1 x}{L_x y} f_y \\ t_2 &= \frac{L_2}{L_x} f_x - \frac{L_2 \left(L_z x + L_x z + L_x L_z \right)}{L_x L_z y} f_y + \frac{L_2}{L_z} f_z \\ t_3 &= \frac{L_3 z}{L_z y} f_y - \frac{L_3}{L_z} f_z \end{aligned} \tag{13}$$

Now, as stated earlier, since this haptic interface has no actuation redundancy in (3 active cables for 3 Cartesian force components); we can only exert ${}^0\mathbf{F}_r$ bounded by all three cable tensions, within the tetrahedron $B_1B_2B_3P$, since cables may only exert tension. In theory, fingertip point P can take any value (subject to cable limits, plus the y position component should be positive in practice), but the resultant force must be contained within the three cables. This is configuration-dependent, and the mathematical determination for TCHI feasible forces is derived below.

Since any feasible (all three cable tensions must be positive) resultant force ${}^0\mathbf{F}_r$ must be bounded by all three cables, if we

project the force vector ${}^0\mathbf{F}_r$ from the fingertip point P back to the XZ plane (y = 0), the force will be feasible only if this intersection point is contained within triangle $B_1B_2B_3$. To derive the intersection point P_{int} (see Figure 4), let $\mathbf{L}_{int}$ be the vector pointing from the finger point P back to the intersection point; $\mathbf{L}_{int}$ is of (unknown) length L, pointing in the unit vector direction ${}^0\hat{\mathbf{F}}_r$ along ${}^0\mathbf{F}_r$. Please see Figure 4 for the intersection point geometry.

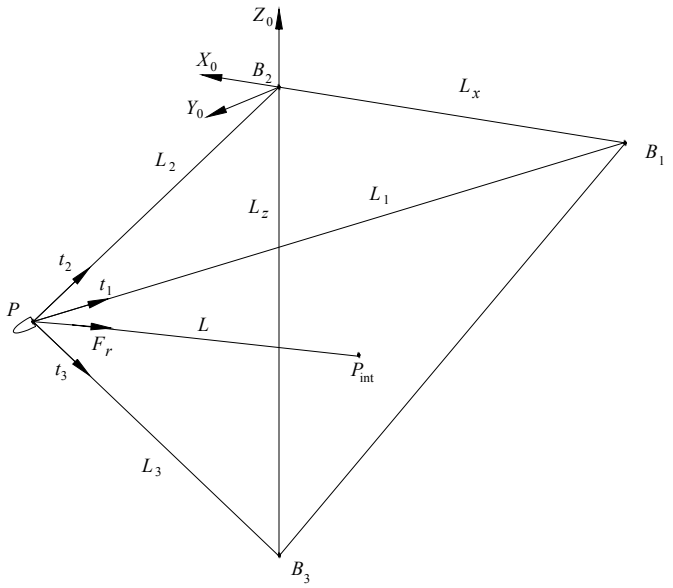

Figure 4. Projection of ${}^0\mathbf{F}_r$ onto *XZ* Plane

The unit vector direction ${}^0\hat{\mathbf{F}}_r$ is:

$$ {}^0\hat{\mathbf{F}}_r = \begin{Bmatrix} \hat{f}_x \\ \hat{f}_y \\ \hat{f}_z \end{Bmatrix} = \frac{1}{\left\| {}^0\mathbf{F}_r \right\|} \begin{Bmatrix} f_x \\ f_y \\ f_z \end{Bmatrix} \tag{14} $$

where $\left\| {}^0\mathbf{F}_r \right\| = \sqrt{f_x^2 + f_y^2 + f_z^2}$ is the Euclidean norm of the resultant force vector. To solve for the unknown length L and the unknown intersection point ${}^0\mathbf{P}_{\text{int}} = \{x_0 \quad 0 \quad z_0\}^T$ given finger position ${}^0\mathbf{P} = \{x \quad y \quad z\}^T$ and given resultant force ${}^0\mathbf{F}_r$, we have the following vector loop closure equation:

$$ {}^0\mathbf{P} + \mathbf{L} = {}^0\mathbf{P}_{\text{int}} $$
$$ \begin{Bmatrix} x \\ y \\ z \end{Bmatrix} + L \begin{Bmatrix} \hat{f}_x \\ \hat{f}_y \\ \hat{f}_z \end{Bmatrix} = \begin{Bmatrix} x_0 \\ 0 \\ z_0 \end{Bmatrix} \tag{15} $$

From the middle equation, the unknown length L to the intersection point from the fingertip point is easily found to be:

$$ L = \frac{-y}{\hat{f}_y} \tag{16} $$

and the remaining unknowns are found by substituting this L into the top and bottom equations of (15):

$$ \begin{aligned} x_0 &= x + L\hat{f}_x \\ z_0 &= z + L\hat{f}_z \end{aligned} \tag{17} $$

The equation for the lower constraint line B_1B_3 is:

$$ Z = \frac{-L_z}{L_x} X - L_z \tag{18} $$

Again, a force will be feasible only if the intersection point P_{int} is contained within base triangle $B_1B_2B_3$. Therefore, any resultant vector force ${}^0\mathbf{F}_r$ is feasible with the TCHI only if all three inequalities in (19) are satisfied (the force is border-line feasible if one or more inequality becomes equal, i.e. one or more cable tension will go to zero, but not negative, in these cases):

$$ \begin{aligned} L &> 0 \\ -\frac{L_x}{L_z}\left(z_0 + L_z\right) &< x_0 < 0 \\ -\frac{L_z}{L_x} x_0 - L_z &< z_0 < 0 \end{aligned} \tag{19} $$

The requirement $L > 0$ is necessary to ensure the force is pointing towards the XZ plane, i.e. if $L < 0$ then at least one negative cable tension will be required. The second two constraints are required to ensure the intersection point P_{int} will lie within triangle $B_1B_2B_3$. The left-hand inequalities of the second two constraints are redundant, i.e. they represent the same linear equation constraint (18). Therefore we can simplify the force-feasible constraints as follows:

$$ \begin{aligned} L &> 0 \\ x_0 &< 0 \\ -\frac{L_z}{L_x} x_0 - L_z &< z_0 < 0 \end{aligned} \tag{20} $$

TCHI SIMULATION EXAMPLES

This section presents three related snapshot examples to demonstrate the required calculations for implementation of the

TCHI. All three examples have the same TCHI at the same fingertip point (that is, with the same three cable lengths), but with different desired Cartesian forces for possible application.

The simulated TCHI design has $L_x = 0.8$ and $L_z = 0.9$ *m* (see Figure 3). The common snapshot position for all three examples has active cable lengths $\mathbf{L} = \{0.4 \quad 0.6 \quad 1.0\}^T$ *m* and fingertip position point ${}^0\mathbf{P} = \{-0.525 \quad 0.275 \quad 0.094\}^T$ (this configuration was developed using FPK but can equally serve as an IPK example).

The three examples below have this same configuration. The three Figures 5 thus have the same kinematics. The heavy blue lines indicate the base and the light red lines are the three active cables. The heavy green line is the Cartesian resultant force to apply. Only example 3 turns out to be feasible since Examples 1 and 2 were designed to require negative cable tension(s).

Example 1

The desired resultant Cartesian fingertip force to be exerted on the human finger is: ${}^0\mathbf{F}_r = \{0.1 \quad 1.0 \quad 0.2\}^T$ *N*. This force is not feasible since the intersection length L is not greater than 0:

$$\begin{aligned} L &= -0.282 \\ x_0 &= -0.553 \\ z_0 &= -0.149 \end{aligned}$$

The required active cable tensions are all negative:

$$\mathbf{T} = \{-1.006 \quad -0.313 \quad -0.604\}^T \ N$$

This case is shown in Figure 5a. The intersection point would lie within the base point triangle, but the force is directed the wrong way, i.e. away from the user.

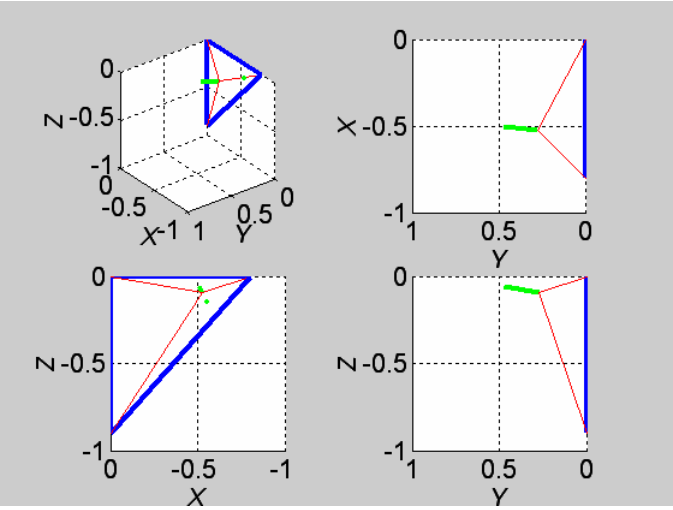

Figure 5a. TCHI Example 1 (length units: m)

Example 2

The desired resultant Cartesian fingertip force to be exerted on the human finger is: ${}^0\mathbf{F}_r = \{-0.5 \quad -1.0 \quad -0.5\}^T$ *N*. This force is not feasible since the intersection point doesn't lie within the base triangle:

$$\begin{aligned} L &= 0.336 \\ x_0 &= -0.662 \\ z_0 &= -0.232 \end{aligned}$$

One of the required active cable tensions is negative:

$$\mathbf{T} = \{1.206 \quad -0.187 \quad 0.938\}^T \ N$$

This case is shown in Figure 5b. The force is directed toward the user, but the intersection point does not lie within the base point triangle (see the green dot in Figure 5b).

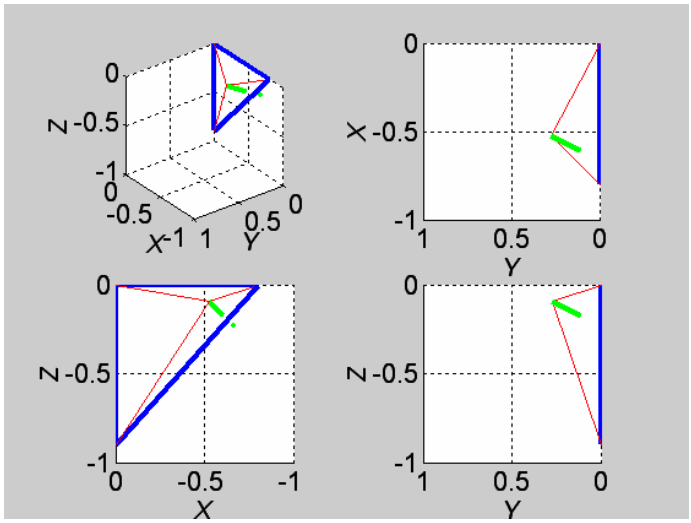

Figure 5b. TCHI Example 2 (m)

Example 3

The desired resultant Cartesian fingertip force to be exerted on the human finger is: ${}^0\mathbf{F}_r = \{-0.3 \quad -0.9 \quad -0.2\}^T$ *N*. This force is feasible since the intersection length L is positive and the intersection point lies within the base triangle:

$$\begin{aligned} L &= 0.296 \\ x_0 &= -0.617 \\ z_0 &= -0.156 \end{aligned}$$

The required active cable tensions are all positive:

$$\mathbf{T} = \{1.010 \quad 0.111 \quad 0.566\}^T \ N$$

This case is shown in Figure 5c. We see the force is directed towards the base and the projection point (green dot in Figure 5c) lies within the base point triangle.

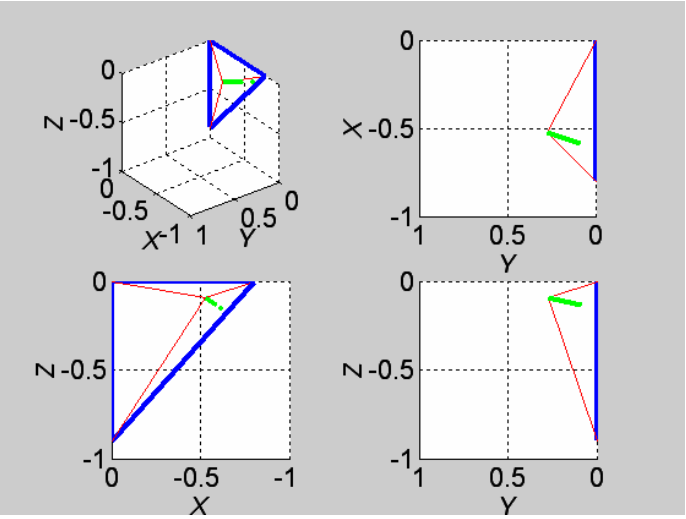

Figure 5c. TCHI Example 3 (m)

TCHI HARDWARE AND CONTROLLER

We have designed the TCHI to match PHANToM® 3.0 specifications. It has been built and controlled at Ohio University. Figure 6 shows our hardware. We specified PITTMAN GM9236S015 24 VDC brush motors, with a continuous torque of 4 oz-in (28.2 mN-m) and equipped with optical encoders with quadrature with a resolution of 500 (x4) CPR. They have a built-in gear ratio 5.9: 1; we would wish smaller gear ratio for less apparent inertia to the user during free motion. For cables we use Teflon-treated super braid fishing line, made with bundles of microfiber tightly woven and coated with polymeric material in order to achieve both high tensile strength and abrasion resistance. We use Aluminum single-wind pulleys, custom designed and machined. Our controller is implemented on a PC in Matlab/Simulink commanding and reading the real-world motors and encoders via a Quanser MultiQ PCI data acquisition board. We use rather standard power supplies and amplifiers.

We have implemented three control modes for feeling virtual surfaces: force control, position control, and combined (not hybrid) force/position control. This work is rather preliminary so we just show one experimental result in Figure 7 where the user moves in the +*y* direction until she feels a virtual wall, under force control. For now the wall is an infinite plane (we've also implemented a corner) and the force ramps up steeply via a polynomial function to a maximum force to indicate a stiff wall.

The units for time in Figures 7 are *msec* and the units for position, Cartesian forces, and tension are *m* and *N*. We see in Figure 7a that the user moved mostly in the +y direction, with small unintentional x and z motions. Upon reaching the virtual wall the y Cartesian force increase greatly (in the negative direction, towards the user as is feasible, see Figure 7b). Figure 7c shows that all cables are in tension for all motion; the minimum allowable tension was 0.22 *N*.

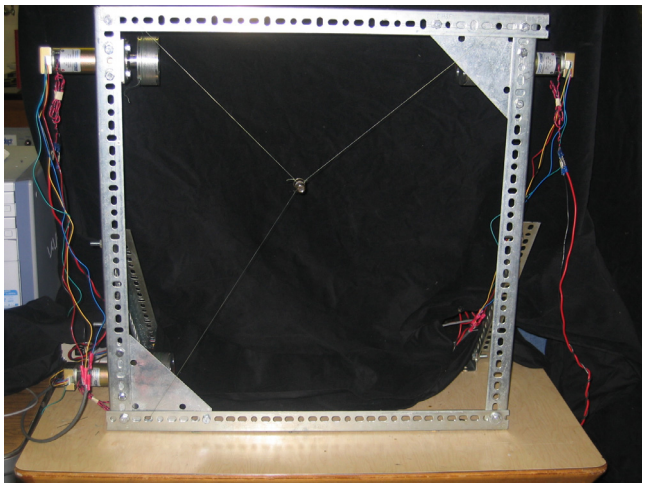

Figure 6. TCHI Hardware

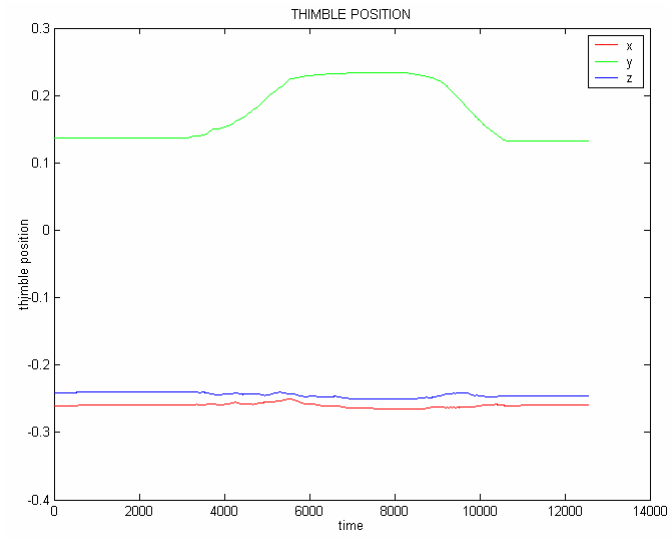

7a. Fingertip Positions (m) vs. time (msec)

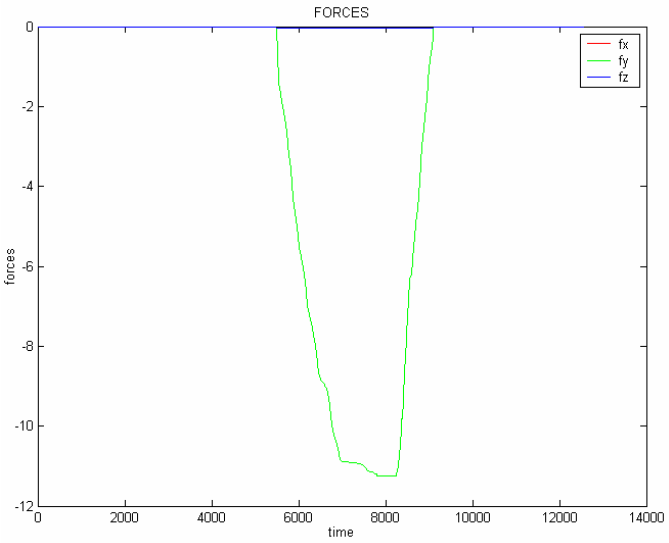

7b. Cartesian Forces (N) vs. time (msec)

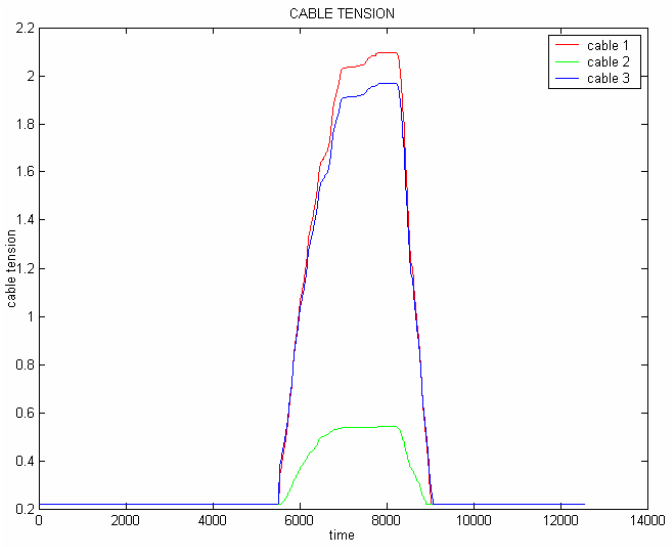

7c. Cable Tensions (N) vs. time (msec)

Figure 7. Preliminary Force Control Experiment

CONCLUSION

This paper has presented our three-cable haptic interface (TCHI) concept, closed-form kinematics and statics solutions, simulation examples, our hardware implementation, plus early experimental results. This device is inspired by the WireMan (Bonivento et al., 1997). Having no actuation redundancy, Cartesian forces can only be applied within the tetrahedron formed by the fingertip point and base cable attachment points. We derived the mathematical conditions for force-feasibility and these are implemented as a check in our controller. This device is suitable for most haptic feedback in our Virtual Haptic Back Project at Ohio University.

ACKNOWLEDGEMENTS

Special thanks to Professor Paolo Gallina of the University of Trieste, Italy, for suggesting this TCHI project. Many thanks also to Professor Alberto Trevisani of the University of Padova, Italy, for lending us the third author for the year as a visiting researcher.

REFERENCES

J.S. Albus, R. Bostelman, and N.G. Dagalakis, 1993, “The NIST ROBOCRANE”, Journal of Robotic Systems, 10(5): 709-724.

C. Bonivento, A. Eusebi, C. Melchiorri, M. Montanari, and G. Vassura, 1997, “WireMan: A Portable Wire Manipulator for Touch-Rendering of Bas-Relief Virtual Surfaces”, Proc. ICAR '97, Monterey.

E. Brau, F. Gosselin, and J.P. Lallemand, 2005, “Design of a Singularity-Free Architecture for Cable-Driven Haptic Interfaces”, Eurohaptics Conference.

P.D. Campbell, P.L. Swaim, and C.J. Thompson, 1995, "Charlotte Robot Technology for Space and Terrestrial Applications", 25th International Conference on Environmental Systems, San Diego.

H.S. Farahani and J. Ryu, 2005, “Design and Control of a Wire-Driven Haptic Device: HapticPen”, ICCAS2005, June 2-5, KINTEX, Gyeonggi-Do, Korea.

P. Gallina, G. Rosati, and A. Rossi, 2001, “3-d.o.f. Wire Driven Planar Haptic Interface”, Journal of Intelligent and Robotic Systems, 32(1):23–36.

M. Ishii and M. Sato, 1994, “A 3D Spatial Interface Device Using Tensed Strings”, Presence-Teleoperators and Virtual Environments, MIT Press, Cambridge, MA, 3(1): 81-86.

S. Kawamura and K. Ito, 1993, “New Type of Master Robot for Teleoperation Using a Radial Wire Drive System”, Proceedings of the IEEE/RSJ International Conference on Intelligent Robots and Systems, Yokohama, Japan, July 26-30, 55-60.

R. Lindemann and D. Tesar, 1989, “Construction and Demonstration of a 9-String 6-DOF Force Reflecting Joystick for Telerobotics”, NASA International Conference on Space Telerobotics, (4): 55-63.

S. Walairacht, Y. Koike, and M. Sato, "A New Haptic Display for Both-Hands-Operation: SPIDAR-8", 1999 IEEE International Symposium on Intelligent Signal Processing and Communication Systems: 569-72.

R.L. Williams II, 1998, "Cable-Suspended Haptic Interface", International Journal of Virtual Reality, 3(3): 13-21.

R.L. Williams II and P. Gallina, 2002, "Planar Cable-Direct-Driven Robots: Design for Wrench Exertion", Journal of Intelligent and Robotic Systems, 35: 203-219.

R.L. Williams II, M. Srivastava, R.R. Conatser Jr., and J.N. Howell, 2004a, "Implementation and Evaluation of a Haptic Playback System", Haptics-e Journal, IEEE Robotics & Automation Society, 3(3): 1-6.

R.L. Williams II, J.S. Albus, and R.V. Bostelman, 2004b, “3D Cable-Based Cartesian Metrology System”, Journal of Robotic Systems, 21(5): 237-257.